Damage induced by femtosecond laser in optical dielectric films

Caihua Huang (黄才华)[1*], Yiyu Xue (薛亦渝)[1], Zhilin Xia (夏志林)[1], Yuan'an Zhao (赵元安)[2], Fangfang Yang (杨芳芳)[1], and Peitao Guo (郭培涛)[1]

[1]*School of Automotive Engineering, Wuhan University of Technology, Wuhan 430070*

[2]*Shanghai Institute of Optics and Fine Mechanics, Chinese Academy of Sciences, Shanghai 201800*

**E-mail: caihuah@tom.com*

Received March 31, 2008

Both the nature of avalanche ionization (AI) and the role of multi-photon ionization (MPI) in the studies of laser-induced damage have remained controversial up to now. According to the model proposed by Stuart *et al.*, we study the role of MPI and AI in laser-induced damage in two dielectric films, fused silica (FS) and barium aluminum borosilicate (BBS), irradiated by 780-nm laser pulse with the pulse width range of $0.01 - 5$ ps. The effects of MPI and initial electron density on seed electron generation are numerically analyzed. For FS, laser-induced damage is dominated by AI for the entire pulse width regime due to the wider band-gap. While for BBS, MPI becomes the leading power in damage for the pulse width τ less than about 0.03 ps. MPI may result in a sharp rise of threshold fluence $F_{\rm th}$ on τ, and AI may lead to a mild increase or even a constant value of $F_{\rm th}$ on τ. MPI serves the production of seed electrons for AI when the electron density for AI is approached or exceeded before the end of MPI. This also means that the effect of initial electron can be neglected when MPI dominates the seed electron generation. The threshold fluence $F_{\rm th}$ decreases with the increasing initial electron density when the latter exceeds a certain critical value.

OCIS codes: 140.3440, 140.3330, 350.1820.

doi: 10.3788/COL20090701.0049.

Laser-induced damage is a key limiting factor for developing high-intensity and ultrashort-pulse laser systems. Researchers have concentrated on this field for many years but no consensus on the mechanism and physical process has been obtained[1−5]. Both the nature of avalanche ionization (AI) and the role of multi-photon ionization (MPI) have remained controversial up to now[6−9]. In previous studies, AI has been regarded as the main power for damage and MPI has served as the seed generator for AI. However, Lenzner's experimental result showed that MPI took over ionization process when the pulse width was short to a certain value[6]. So it is necessary to understand the laser-induced damage mechanism. In this letter, based on the model proposed by Stuart *et al.*[10], we numerically analyze the role of MPI and the nature of AI in fused silica (FS) and barium aluminum borosilicate (BBS) dielectric films irradiated by 780-nm laser pulse with the pulse width range of $0.01 - 5$ ps. Also, the initial electron density is considered as an important factor which competes with MPI to provide initial seed electrons for AI.

Bloembergen summarized the classical literature and provided electron density rate equation to explain the damage mechanism in optical dielectrics[11,12]:

$$\partial N/\partial t = \eta(E)N + (\partial N/\partial t)_{\rm PI} - (\partial N/\partial t)_{\rm loss}. \quad (1)$$

The term on the left-hand side is the rate of increase in the electron density N. The first term on the right-hand side represents avalanche ionization, $\eta(E)$ is the avalanche coefficient, and E is the electric field strength. The second term is the photon ionization contribution. The third term is the loss due to electron diffusion, recombination, etc.

In terms of Bloembergen's point, the optical dielectric damage only relates to MPI, AI, and electronic loss. Bloembergen and Du *et al.* pointed out that the electronic loss was negligible during the duration of a short pulse[10,11].

Based on this principle, Stuart *et al.* derived a simple rate equation for the evolution of the free electron density $N(t)$ in dielectrics exposed to intense laser radiation[10],

$$\mathrm{d}N(t)/\mathrm{d}t = \alpha I(t)N(t) + \sigma_m I(t)^m. \quad (2)$$

The first term on the right-hand side represents AI, where $I(t)$ is the laser pulse intensity. The second term represents MPI, in which σ_m is the m-photon absorption cross section with the smallest m satisfying $m\hbar\omega \geq \Delta$, where ω is the laser frequency, Δ is the band-gap energy of the material. The energy of the free electrons heated by the laser is subsequently transferred to the lattice. This energy transfer leads to the ablation of the heated zone, which is the major manifestation of femtosecond optical damage.

The exponential pulse laser function is

$$I(t) = \begin{cases} I_0 \exp(t/\tau_0) & t \leq 0 \\ I_0 \exp(-t/\tau_0) & t \geq 0 \end{cases}, \quad (3)$$

where I_0 is the peak intensity of laser pulse, the relation between the laser pulse duration τ and the characteristic parameter τ_0 is $\tau = 2\tau_0 \ln 2$. The relevant parameters are selected as follows: $\alpha_{\rm FS} = 3.3$ cm^2/J and $\alpha_6 = 6 \times 10^{10}$ ps^{-1}(cm^2/J)^6 for FS; $\alpha_{\rm BBS} = 1.2$ cm^2/J and $\alpha_3 = 7 \times 10^{17.1}$ ps^{-1}(cm^2/J)^3 for BBS. The laser wavelength $\lambda = 780$ nm. The initial electron density N_i is postulated to be 10^{10} cm^{-3} and the threshold electron density $N_{\rm th} = 10^{21}$ cm^{-3}. The band-gap energies of FS and BBS are 9 and 4 eV, respectively[6,13].

© 2009 Chinese Optics Letters

The threshold fluence F_{th} increases with the pulse width τ broadening, as shown in Fig. 1. The two curves reveal the important similarity and difference for the two dielectric films. The similarity is that the increasing rate of F_{th} on τ is higher for shorter pulse than for longer pulse. While the difference lies in the different slope of the two curves. In fact, the parameters used for calculation in Eq. (2) are closely relevant to the band-gap energy. According to Ref. [2], the difference of band-gap energy should account for the characteristics mentioned above. For short pulse duration studied in this letter, $\tau = 0.01 - 5$ ps, the wider band-gap means higher threshold, which agrees well with Yuan's conclusion[2]. Additionally, the wider band-gap leads to the more rapid increasing rate for shorter pulse duration and the slower one for longer pulse duration. The threshold fluence values from earlier work in this pulse width regime are also shown in Fig. 1. By comparison, it can be seen that our data agree well with the earlier results.

The effects of AI and MPI on free electron evolution is reflected by $\log(\text{eD}_{\text{AI}}/\text{eD}_{\text{MPI}})$, here eD_{AI} and eD_{MPI} represent the electron densities provided by AI and MPI, respectively. The curves of $\log(\text{eD}_{\text{AI}}/\text{eD}_{\text{MPI}})$ on τ are shown in Fig. 2. The rising tendency of $\log(\text{eD}_{\text{AI}}/\text{eD}_{\text{MPI}})$ means the increasing influence of AI and decreasing effect of MPI with the pulse duration τ broadening.

However, there are differences about FS and BBS due to the different band-gap energies of the two dielectrics. For FS, the electron density provided by AI is $1 - 9$ orders of magnitude higher than that of MPI, which means that the laser-induced damage in FS is dominated by AI, which agrees well with the results of Refs. [6,7]. While for BBS, when τ is less than about 0.03 ps, $\log(\text{eD}_{\text{AI}}/\text{eD}_{\text{MPI}}) < 0$, which suggests that MPI plays a leading role in electron ionization. When $\tau > 0.03$ ps, AI exceeds MPI and becomes the main power for ionization. The narrower band-gap means more easy multi-photon absorption and consequently leads the greater effect of MPI. That is why the MPI is more remarkable for BBS.

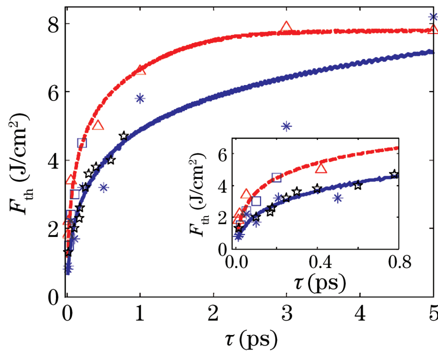

Fig. 1. Threshold fluence F_{th} versus pulse width τ for FS and BBS thin films. Triangles and stars represent the experimental data for FS and BBS respectively in Ref. [6]; squares represent the experimental data for FS in Ref. [7]; pentagrams represent the experimental F_{th} for MgF_2 in Ref. [8].

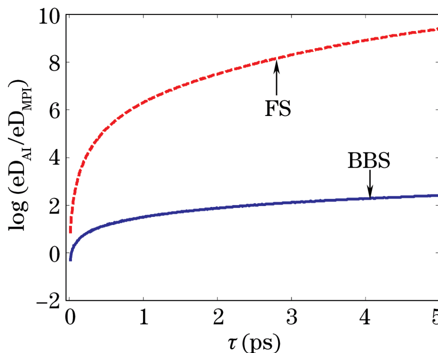

Fig. 2. Dependence of $\log(\text{eD}_{\text{AI}}/\text{eD}_{\text{MPI}})$ on τ for FS and BBS.

Combined with variation tendency of F_{th} on τ, AI and MPI reflect different effects on F_{th}. The dominant AI means the mild variation of F_{th} on τ. With the decrease of pulse duration τ, the effect of MPI is enhanced and the variation of F_{th} on τ is remarkable. These analyses may suggest that MPI results in a sharp rise of F_{th} on τ, and AI results in a mild increase or even a constant value of F_{th} on τ.

The initial electron is an important factor which may compete with MPI to provide seed electrons for AI. In principle, the influence of the initial electrons descends with the decrease of pulse duration. By comparing the final electron density of MPI with the initial electron density N_i, it cannot determine the main contributor for seed electrons for AI. Figure 3 shows the logarithm relation of $\text{eD}_{\text{MPI}}/N_i$ with τ. Taking FS as an example, though the electron density of MPI exceeds N_i for τ less than 5 ps, this does not mean that MPI is the main channel for the seed electron generation.

However, it can be determined that MPI is the dominant seed electron generation channel if the electron density of MPI approaches or exceeds the electron density of AI before the end of MPI. This qualitative criterion implies that the dominant role of MPI for seed generation means the negligible effect of initial electron. Figure 4 shows the ionization status in FS when MPI dominates the seed electron generation for $\tau = 0.1$ ps. The pulse duration is far less than the case of 5 ps reflected in Fig. 3.

The effect of initial electron density N_i on the threshold fluence F_{th} is worth discussing here. F_{th} keeps a constant value for a certain pulse width when N_i ranges from zero to a critical value. Once N_i exceeds the critical value, F_{th} begins to decrease with the increase of N_i. Here it should be noted that the critical value is not a constant, but will increase with the decrease of pulse width τ. Figures 5 and 6 show the influence of N_i and τ on F_{th} for FS and BBS, respectively. It is clear that the critical value of BBS is higher than that of FS, which indicates that the narrower band-gap means the less effect of N_i on F_{th}.

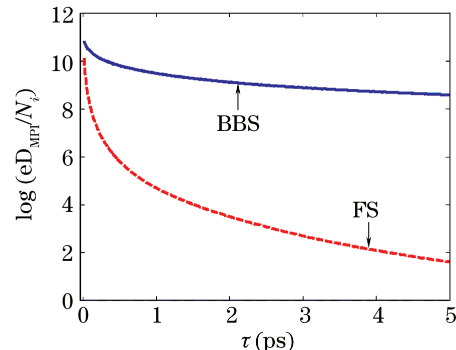

Fig. 3. Dependence of $\log(\text{eD}_{\text{MPI}}/N_i)$ on τ for FS and BBS.

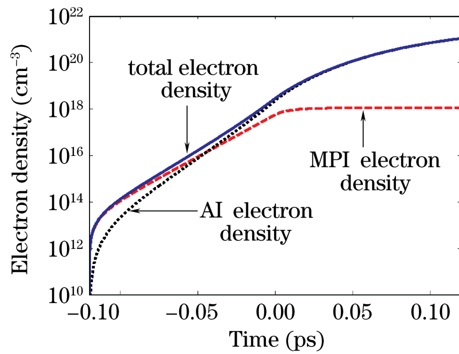

Fig. 4. MPI dominates the seed electron generation in FS for $\tau = 0.1$ ps.

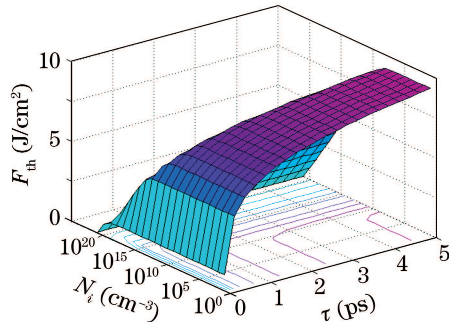

Fig. 5. Effect of N_i and τ on $F_{\rm th}$ for FS.

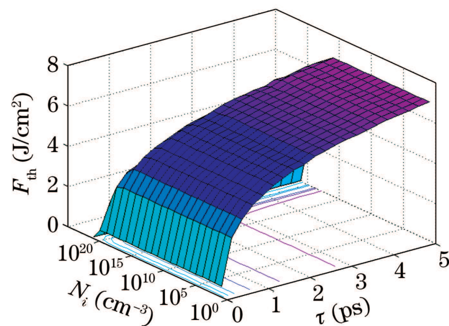

Fig. 6. Effect of N_i and τ on $F_{\rm th}$ for BBS.

In conclusion, the wider band-gap means higher threshold for the short pulse duration discussed in this letter. The wider band-gap leads to a more rapid increasing rate of threshold for shorter pulse duration and a slower one for longer pulse duration. For FS, AI dominates the ionization process for the entire pulse width regime studied due to the wider band-gap. While for BBS, the laser-induced damage is still dominated by AI for longer pulse width but MPI takes over for shorter pulse duration. The effect of AI and MPI on the threshold fluence $F_{\rm th}$ is contrary. Namely, MPI may result in a sharp rise of $F_{\rm th}$ on τ, and AI may result in a mild increase or even a constant value of $F_{\rm th}$ on τ. The initial electrons compete with MPI to provide seed electrons for AI. MPI serves the production of seed electrons for AI when MPI approaches or exceeds the electron density of AI before the end of MPI. This also means that the effect of initial electron can be neglected when MPI dominates the seed electron generation. When the initial electron density N_i exceeds a certain critical value, $F_{\rm th}$ decreases with the increasing N_i. Additionally, the narrower band-gap means the less effect of N_i on $F_{\rm th}$.

This work was supported by the National Natural Science Foundation of China (No. 10804090 and 60708004) and the Wuhan University of Technology Foundation (No. xjj2007031).

References

1. Y. Li, F. Ma, N. Dai, G. Yang, and P. Lu, Chinese J. Lasers (in Chinese) **34,** 1009 (2007).
2. L. Yuan, Y. Zhao, H. He, and J. Shao, Chin. Opt. Lett. **5,** S257 (2007).
3. Y. Cui, H. Yu, Y. Zhao, Y. Jin, H. He, and J. Shao, Chin. Opt. Lett. **5,** 680 (2007).
4. J. G. Fujimoto, J. M. liu, and E. P. Ippen, Phys. Rev. Lett. **53,** 1837 (1984).
5. B. Rethfeld, Phys. Rev. Lett. **92,** 187401 (2004).
6. M. Lenzner, J. Krüger, S. Sartania, Z. Cheng, Ch. Speilmann, G. Mourou, W. Kautek, and F. Krausz, Phys. Rev. Lett. **80,** 4076 (1998).
7. A. Kaiser, B. Rethfeld, M. Vicanek, and G. Simon, Phys. Rev. B **61,** 11437 (2000).
8. H. Sun, T. Jia, C. Li, X. Li, S. Xu, D. Feng, X. Wang, X. Ge, and Z. Xu, Solid State Commun. **141,** 127 (2007).
9. S. Xu, T. Jia, X. Li, D. Feng, H. Sun, C. Li, X. Wang, H. Kuroda, R. Li, and Z. Xu, Jpn. J. Appl. Phys. **44,** 8201 (2005).
10. B. C. Stuart, M. D. Feit, A. M. Rubenchik, B. W. Shore, and M. D. Perry, Phys. Rev. Lett. **74,** 2248 (1995).
11. N. Bloembergen, IEEE J. Quantum Electron. **10,** 375 (1974).
12. D. Du, X. Liu, G. Korn, J. Squier, and G. Mourou, Appl. Phys. Lett. **64,** 3071 (1994).
13. Z. Xia, J. Shao, and Z. Fan, Chinese J. Mater. Res. (in Chinese) **20,** 581 (2006).